Structure and Spectroscopic Properties of Iron Oxides with the High Content of Oxygen: FeOn and FeOn− (n=5−12)

ARTICLE *in* THE JOURNAL OF PHYSICAL CHEMISTRY A · SEPTEMBER 2010

Impact Factor: 2.69 · DOI: 10.1021/jp1050645 · Source: PubMed

4 AUTHORS, INCLUDING:

G. L. Gutsev
Flolida A&M University
219 PUBLICATIONS **3,797** CITATIONS
SEE PROFILE

Charles Weatherford
Florida A&M University
119 PUBLICATIONS **458** CITATIONS
SEE PROFILE

Structure and Spectroscopic Properties of Iron Oxides with the High Content of Oxygen: FeO_n and FeO_n^- ($n = 5-12$)

G. L. Gutsev,*,† C. A. Weatherford,† K. Pradhan,‡ and P. Jena‡

Department of Physics, Florida A&M University, Tallahassee, Florida 32307, and Department of Physics, Virginia Commonwealth University, Richmond, Virginia 23284

Received: June 2, 2010; Revised Manuscript Received: July 7, 2010

The electronic and geometrical structures of oxygen-rich neutral and negatively charged FeO_5, FeO_6, FeO_7, FeO_8, FeO_9, FeO_{10}, FeO_{11}, and FeO_{12} clusters were obtained using density functional theory with generalized gradient approximation. With the exception of FeO_{11} and FeO_{12}, all clusters are found to possess a large number of isomers composed of oxo, peroxo, superoxo, and ozonide fragments that are closely spaced in total energy, especially for $n = 7$ and 8. The preferable structures of FeO_{12} are composed of superoxo groups with different orientations. All the neutral species possess rather large electron affinities, which range from 3.24 eV (FeO_8) to 3.95 eV (FeO_5). Although all of the lowest energy states were found to possess positive vibrational frequencies and thus are geometrically stable, the states are thermodynamically unstable against dissociation to $FeO_4 + (n - 4)/2\ O_2$ for $n = 6$, 8, 10, and 12 and $FeO_5 + (n - 5)/2\ O_2$ for $n = 7$, 9, and 11. In particular, the decay of FeO_{12} is exothermic by 34 kcal/mol.

Introduction

Oxides of transition metals (TM) do play an important role in various catalytic and biological processes and consequently are the subject of numerous experimental and theoretical studies.[1] Iron oxides are of a special interest because of their use in a number of technological processes, such as catalyzed oxidation of carbon monoxide,[2] and in the assembling of fuel cells based[3] on converting water to hydrogen since water dissociates on iron clusters.[4] In addition, the corrosion processes are considered to be accompanied[5] by the formation of iron oxides.

The smallest iron oxide, a FeO dimer, is one of the most studied species among all TM oxides both experimentally[6] and theoretically.[7] Yet, there is controversy over the assignment of the ground state of the FeO^- anion. According to a recent theoretical study performed at a rather extensive CASPT2 level,[8] the ground state of the anion is $^6\Sigma^+$, which was contested by the experimentalists[9] who interpreted their laser photodetachment spectrum as originating from a $^4\Delta$ state. This is also in accordance with a number of other theoretical papers that dealt with the anion. The controversy stems from the closeness of the total energies of the $^4\Delta$ and $^6\Sigma^+$ states of FeO^-.

Iron dioxide FeO_2 and its anion have been studied using a number of experimental methods such as laser photodetachment spectroscopy,[6g−i] IR spectroscopy,[10] and Mössbauer spectroscopy.[11] It was established on the basis of the obtained experimental data and the results of theoretical studies[6f,7c,10c,12] that the ground state of FeO_2 is $^3B_1$ with the oxo-type bonding. Both peroxo [or side-on $Fe(O_2)$] and superoxo (or end-on FeOO) complexes were found to be appreciably higher in total energy.

Iron trioxide FeO_3 was identified[6g,h] from the photoelectron spectra as possessing D_{3h} symmetry, whereas its excited state with a $(O_2)FeO$ geometrical configuration was observed[13] in the IR spectra recorded for FeO_3 trapped inside solid argon. The results of theoretical studies[7i,14] have confirmed that the FeO_3 ground-state geometry is an equilateral triangle and its ground state is A_1'.

The ground state of iron tetraoxide is a matter of controversy. Although pure density functional theory (DFT) methods have predicted[15] a tetrahedral oxo-geometry for the ground singlet state of FeO_4, ab initio and hybrid HF-DFT methods favored[16] a peroxo-state of C_{2v} symmetry. However, the difference between total energies of these two states is only 0.2 eV at the BPW91/6-311+G* level. Thus, the two states can be considered as nearly degenerate in total energy, which is in agreement with assigning[17] the oxidation number of 6 to Fe in iron oxides.

It was rather surprising when Wang et al.[18] managed to produce CuO_n^- anions for n up to 6 and measured their photoelectron spectra. According to the experimental data, the extra electron binding energies are nearly the same (~3.2 eV) for all $n = 3-6$. Subsequent theoretical studies[19] have confirmed the stability of the neutral and negatively charged CuO_n complexes and found that these complexes do possess a plenty of states, which are closely spaced in total energy and whose geometries are formed by different combinations of ozonide, peroxo, and supero fragments. Neutral CuO_4 and CuO_5 have recently been identified[20] in solid argon and were found to have the ground state configurations of the double peroxo type for CuO_4 (D_{2h} symmetry) and the peroxo-ozonide type for CuO_5 (C_{2v} symmetry). Another surprising result is the recent discovery[21] of highly oxygen rich ScO_4 (biperoxide), ScO_6 (triperoxide), and ScO_8 (peroxo-biozonide) species in solid argon.

Since the oxidation number of Fe is twice as large[17] as that of Sc, the above results raise an interesting question: can a Fe atom bind to more oxygen atoms than Sc? Unfortunately, there are no experimental data on the structure of iron oxides FeO_n for $n > 4$. On the theoretical hand, Atanasov[15b] has predicted a bisuperoxo structure $(O_2)_2FeO$ for FeO_5, whereas FeO_5 and FeO_6 species were proposed to be O_2 adducts of iron trioxide and tetroxide, respectively, on the basis of an ab initio molecular dynamics study.[22]

* To whom correspondence should be addressed. E-mail: gennady.gutsev@famu.edu.
† Florida A&M University.
‡ Virginia Commonwealth University.

10.1021/jp1050645
Published on Web 07/29/2010

TABLE 1: Comparison of Geometry and Energetics of Oxo and Peroxo States of FeO_n and FeO_n^- Obtained at Different Levels of Theory with the 6-311+G(3df) Basis[a]

		BPW91	PBE*2	TPSS*2	B3PW91	B3LYP
FeO_4	T_d $^1A_1$ E_{tot}	0.73272	0.09405	0.68617	0.32547	0.50138
	r(Fe−O)	1.5942	1.5931	1.5903	1.5651	1.5739
	ZPVE	0.353	0.354	0.357	0.376	0.370
	C_{2v} $^1A_1$ E_{tot}	0.73042	0.09246	0.68787	0.36150	0.53642
	r_1(Fe−O)	1.5676	1.5667	1.5644	1.5383	1.5458
	r_2(Fe−O)	1.7760	1.7746	1.7662	1.7482	1.7602
	r(O−O)	1.3810	1.3771	1.3922	1.3617	1.3745
	ZPVE	0.335	0.336	0.339	0.356	0.349
	$-\Delta E_{tot}(T_d - C_{2v})$	**+0.044**	**+0.025**	**−0.064**	**−1.000**	**−0.974**
FeO_4^-	D_{2d} $^2B_2$ E_{tot}	0.86711	0.22796	0.82327	0.48862	0.66897
	r_1(Fe−O) = r_2(Fe−O)	1.6287	1.6276	1.6248	1.6005	1.6094
	ZPVE	0.319	0.323	0.327	0.340	0.340
	C_{2v} $^2A_2$ E_{tot} au	0.83743	0.19888	0.79825	0.49653	0.67637
	r_1(Fe−O)	1.6105	1.6092	1.6078	1.5851	1.5931
	r_2(Fe−O)	1.8077	1.8059	1.7996	1.7853	1.7974
	r(O−O)	1.4423	1.4387	1.4525	1.4128	1.4275
	ZPVE	0.297	0.298	0.301	0.318	0.311
	$-\Delta E_{tot}(D_{2d} - C_{2v})$	+0.786	+0.766	+0.654	−0.215	−0.201
	EA_{ad}	**3.691**	**3.675**	**3.696**	**3.712**	**3.846**
adiabatic BE ($D_{2d} \rightarrow T_d$)		3.691	3.675	3.761	4.475	4.590
adiabatic BE ($C_{2v} \rightarrow C_{2v}$)		2.950	2.934	3.042	3.712	3.846
vertical BE ($D_{2d} \rightarrow T_d$)[b]	2S + 1 = 1	3.759	3.747	3.837	4.565	4.682
	2S + 1 = 3	4.750	4.755	4.698	5.305	5.063
vertical BE ($C_{2v} \rightarrow C_{2v}$)[c]	2S + 1 = 1	3.074	3.057	3.170	3.853	3.980
	2S + 1 = 3	4.901	3.807	3.739	4.084	4.217

[a] E_{tot} in au, all E_{tot} entries begin with −1564; bond length r_i are in Å; all other values are in eV; the positive value of $-\Delta E_{tot}$ means that the second state in the parentheses are above the first state; BE denotes the binding energy of the extra electron; and 2S + 1 = 1 and 2S + 1 = 3 denotes the spin multiplicities of the neutral final states formed after the extra electron detachment. The number of basis functions is 237. [b] Experimental value 3.84(4) eV. [c] Experimental value 3.30(4) eV.

The present paper is aimed at a systematic search of geometrically stable isomers of FeO_n and FeO_n^- for $n = 5-12$ using density functional theory with generalized gradient approximation (DFT-GGA). First, we performed calibration calculations on FeO_4, for which experimental data are available, in order to evaluate the performance of several methods that could be used in computations. Next we performed extensive optimizations of FeO_n with topologies presented by different combinations of oxo, peroxo, superoxo, and ozonide fragments. We also computed electron affinities of the lowest energy neutral species and energies required for the dissociation of the neutral and negatively charged FeO_n species.

Calibration using FeO_4 and FeO_4^-. Computations were performed using the Gaussian 03[23] program systems using the 6-311+G* basis set[24] [Fe:(15s11p6d1f/10s7p4d1f); O:(12s6p1d/5s4p1d)] for preliminary optimizations and the 6-311+G(3df) basis [Fe:(15s11p6d3f1g/10s7p4d3f1g); O:(12s6p3d1f/5s4p3d1f)] for the final optimizations. In order to gain insight into the performance of different methods, we chose FeO_4 because of its controversial assignment of the ground state and the availability of the photoelectron spectrum for the FeO_4^- anion. Our calibration calculations are performed using the pure DFT BPW91[25,26] and PBEPBE[27] methods, the hybrid HF-DFT[28−30] B3PW91 and B3LYP methods, and the recently developed[31] τ-dependent gradient-corrected TPSSTPSS approach.

The results of our computations for neutral and singly negatively charged FeO_4 corresponding to oxo (T_d) and peroxo (C_{2v}) isomers using the 6-311+G(3df) basis set are given in Table 1. The symmetry of the FeO_4^- anion reduced to D_{2d} without significant distortion of the T_d nuclear frame. We present equilibrium bond distances r(Fe−O) and r(O−O), zero point vibrational energies (ZPVE), differences in total energies $\Delta E_{tot}(T_d - C_{2v})$ for the neutral species and $\Delta E_{tot}(D_{2d} - C_{2v})$ for the anions, adiabatic electron affinities of the neutral defined as $EA_{ad} = E_{tot}$(neutral) − ZPVE(neutral) − E_{tot}(anion) + ZPVE(anion). Here E_{tot}(neutral) and E_{tot}(anion) are total energies of the corresponding lowest total energy states obtained with a given method. Also presented are the adiabatic and vertical binding energies (BE) of the extra electron in the anion. The vertical binding energies do correspond to the features observed in the experimental photodetachment spectra.

As follows from the table, the BPW91, PBEPBE, and TPSSTPSS methods do provide quite similar results, which are somewhat different from those obtained using the HF-DFT methods. In particular, bond distances are smaller by ∼0.02 Å and the neutral $^1A_1$ (C_{2v}) state is significantly lower in total energy than the corresponding $^1A_1$ (T_d) state at both HF-DFT levels. The anion states show same pattern. The neutral $^1A_1$ states are practically degenerate and the oxo-isomer of the anion is well below in total energy than the peroxo-isomer at the BPW91, PBEPBE, and TPSSTPSS levels. The BPW91 difference of 0.2 eV obtained previously with the 6-311+G* basis decreases to 0.044 eV when the 6-311+G(3df) basis set used. In order to explore the influence of the basis extensions on the relative positions of the FeO_4 T_d and C_{2v} states, we chose Dunning's[32] cc-pVTZ (188 basis functions), cc-pVQZ (324 basis functions), and cc-pV5Z (517 basis functions) sets since these basis sets do contain more primitive Gaussian functions than the 6-311+G(3df) basis. The $\Delta E_{tot}(T_d - C_{2v})$ difference, +0.057 eV (TZ), +0.046 eV (QZ), and +0.318 eV (5Z) has to be compared with +0.044 eV obtained with the 6-311+G(3df) basis set. Taking into account that computations using the cc-pV5Z basis are extremely time-consuming, the choice of the 6-311+G(3df) basis appears to be a reasonable one.

Since the DFT and HF-DFT methods favor different lowest energy states, we compared their predictions for the anion extra

electron binding energies with experiment. The DFT methods predict the first transition to be within the range of 3.07−3.17 eV and correspond to the $C_{2v} \rightarrow C_{2v}$ doublet-singlet transition. These values have to be compared with the experimental value[6g,h] of 3.30(4) eV. The second experimental feature at 3.84(4) eV compares well with the energy of the $D_{2d} \rightarrow T_d$ doublet-singlet transition which ranges from 3.69 to 3.76 eV (see Table 1). The B3PW91 and B3LYP values are 3.85 and 3.98 eV for the $C_{2v} \rightarrow C_{2v}$ transition and 4.56 and 4.68 eV for the $D_{2d} \rightarrow T_d$ transition. That is, both are well off the experimental value of 3.30(4) eV.

In order to gain insight about the energetics of excited states at the neutral C_{2v} geometry, we performed time-dependent DFT[33] computations at the BPW91/6-311+G(3df) level. We found that there are two states ($^3A_1$ and $^3A_2$), which are above the initial $^1A_1$ state by 0.53 and 0.79 eV, respectively. Therefore, these states may be responsible for the second peak in the experimental spectrum around 4 eV. Thus, the origin of the second peak is not clear: or is it due to the excited neutral C_{2v} states, or it is due to the presence of the D_{2d} anion isomer in the measured sample gas?

Note that the performance of the BPW91 functional seems to be quite similar to that of the PBEPBE and TPSSTPSS functionals. Since the BPW91 functional is preferred[34] in vibrational frequency calculations of pure iron clusters and is faster[35] than the TPSSTPSS method, we choose the BPW91 method for the remainder of this work. It should be mentioned that the BPW91 approach has recently been found to be preferable in the study of Mo and W oxides.[36] The BPW91 performance was also found to be the best, if compared to the performance of the MRCI method, in computations[12a] of FeO_2.

Results and Discussion

First we perform a search of the lowest energy states of FeO_n and FeO_n^- for $n = 5-12$, keeping in mind that a number of different oxygen configurations is possible. They include an oxo-form, where an oxygen atom binds dissociatively, peroxo- and superoxo-forms, where two oxygen atoms bind associatively, and ozonide form O_3, where three oxygen atoms bind associatively. No bound oxygen rings similar to those found[37] in CO_n species for $n > 3$ was found in our optimizations of FeO_n and FeO_n^-, which is consistent with the van der Waals interactions[38] of O_2 dimers. In particular, the O_4 ring did break into two peroxo group (e.g., in FeO_5) or one O_2 did dissociate (e.g., in FeO_5^-). Next, we will compute the adiabatic electron affinities and, finally, estimate the thermodynamic stability of the lowest energy species for each n.

Geometrical Configurations. The results of our optimizations of FeO_5 and its anion are presented in Figure 1. Both ground state geometries do have one superoxo O_2, followed by isomers possessing two peroxo, one peroxo and one superoxo, and a peroxo and an ozonide unit. The Fe−O and O−O distances shown in the Figure are typical for all iron oxides considered in this work, namely: oxo Fe−O ≈ 1.60−1.65 Å, peroxo Fe−O ≈ 1.75−1.90 Å, superoxo Fe−O ≈1.85−2.05 Å, peroxo O−O ≈ 1.32−1.40 Å, superoxo O−O ≈ 1.22−1.28 Å; the Fe−O and O−O distances for ozonide fragments are similar to those for superoxo O_2 groups. The spin-multiplicity ordering of the states possessing the same geometrical configuration is often not the same in different topology series. For example, the lowest energy state with one peroxo group is a singlet, while the lowest energy state in the peroxo-ozonide series is a quintet. In all singlet states (the notable exception is FeO_4), the Fe atom carries some excess spin density. This

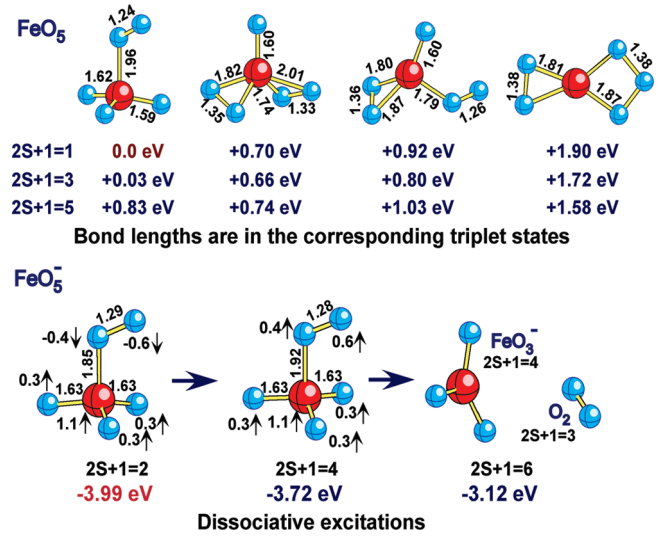

Figure 1. Geometrical configurations of different isomers of FeO_5 and its anion together with the energy shifts with respect to the neutral ground state with the spin multiplicity $2S + 1 = 1$. Bond lengths are in Å, excess spin densities on atoms are in e.

requires the use of spin-unrestricted formalism for singlet states and the corresponding guesses where spin-up and spin-down electronic densities are split.

The distribution of excess spin densities on atoms in the FeO_5^- anion is rather typical for all other FeO_n and FeO_n^-: the excess spin densities are coupled antiferromagnetically in the low-spin states and ferromagnetically in the high-spin states. Spin excitations of geometrically stable states do often result in dissociation of the initial species by producing one or more O_2 dimers. In the case of FeO_5^-, spontaneous dissociation to the FeO_3^- anion ($^4A_1'$, D_{3h}) and an O_2 dimer ($X\ ^3\Sigma_g^-$) occurs after the doublet ground state is excited to a quartet state and the latter is exited to a sextet state.

Figure 2 presents geometrical configurations corresponding to the lowest energy states for both FeO_6 and FeO_6^-. The ground states possess the same topology with two peroxo groups. Among other configurations, a 3-peroxo configuration corresponds to the lowest energy excited state. Transformations of peroxo groups into superoxo groups lead to a substantial increase in total energy of the corresponding states. A biozonide isomer is the less favorable in total energy.

Any isomer of FeO_7 must have at least one oxo or ozonide unit since the number of oxygen atoms is odd. No stable trioxo isomer is found. Total energies of the lowest energy isomers presented in Figure 3 are rather close to each other for the states with different geometrical configurations. The lowest energy state contains three superoxo groups and is lower in total energy than the state with the geometrical configuration containing two ozonide groups by only 0.34 eV. The ground state of the anion has the same topology as the ground state of the neutral but its superoxo groups possess a different orientation.

FeO_8 has the largest number of different topologies in the entire series. They include combinations containing one oxo-O, which must be accompanied by an ozonide, as well as biozonide, tetra-peroxo, and tetra-superoxo configurations. As is seen from Figure 4, the spin multiplicity of the lowest energy states for each topology ranges from 1 to 5. There are a large number of states, which are spaced within 1 eV energy gap. The lowest energy state of FeO_8 contains one superoxo and three peroxo O_2, while the anion has two peroxo and two superoxo groups. Note that the neutral has a singlet lowest energy state

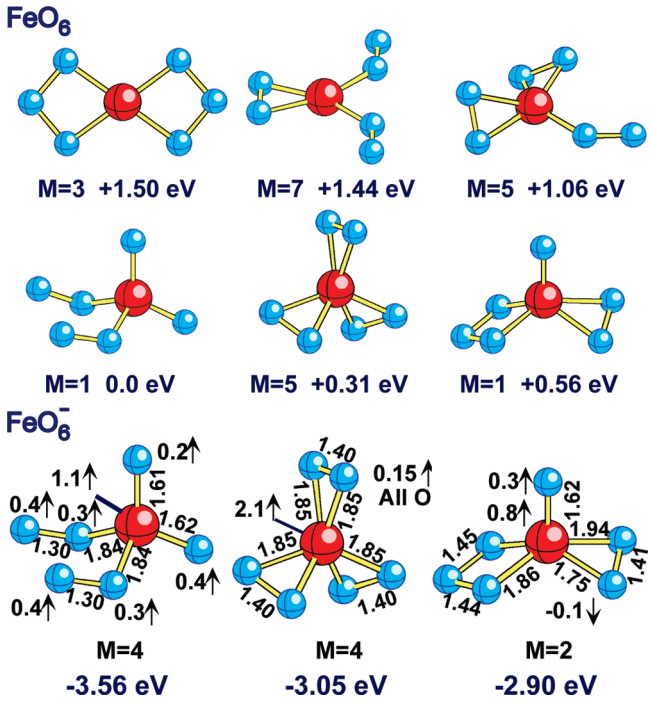

Figure 2. Geometrical configurations of different isomers of FeO_6 and its anion together with the energy shifts with respect to the neutral ground state with the spin multiplicity $M = 2S + 1 = 1$. Bond lengths are in Å, excess spin densities at atoms are in e.

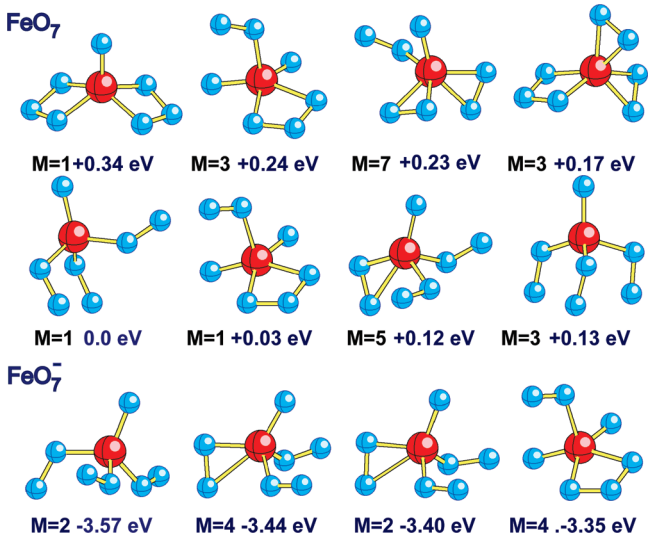

Figure 3. Geometrical configurations of the lowest energy isomers of FeO_7 and its anion together with the energy shifts with respect to the neutral ground state with $2S + 1 = 1$.

whereas the lowest energy state of the FeO_8^- anion is a sextet. The doublet and quartet anion states containing an ozonide group are nearly degenerate in total energy with the lowest energy anion state, whereas the singlet neutral state with the same topology is above the ground state by 0.53 eV. A singlet state with a biozonide geometry is the highest in total energy.

A geometrical configuration of FeO_9 must contain either oxo or ozonide fragment, and this restriction reduces the number of combinations with respect to that in the previous case. No stable state with a bioxo topology is found. The lowest energy neutral state is a triplet and its geometrical configuration contains one peroxo and three superoxo groups. Two singlet states with 2-ozonide and 3-ozonide geometries are higher in total energy

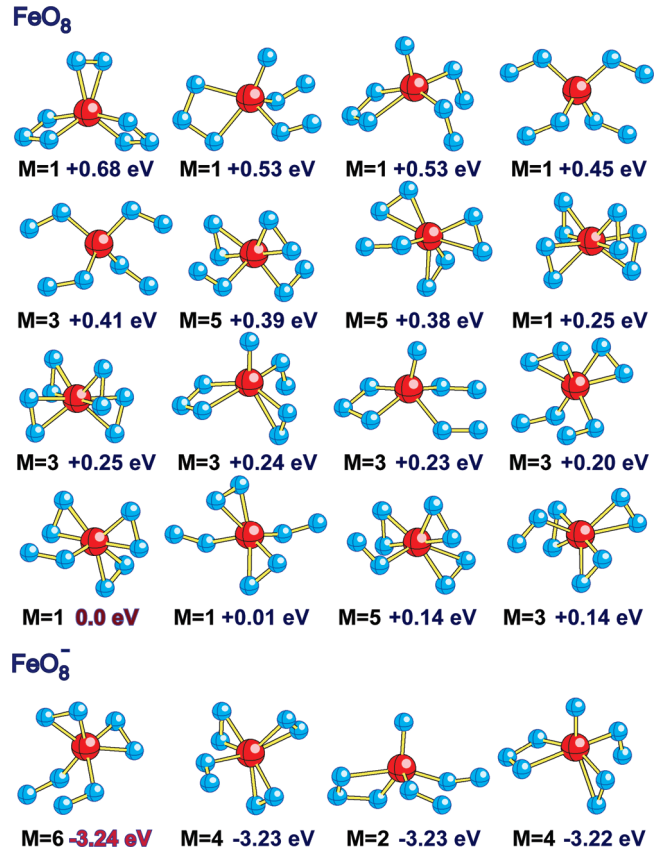

Figure 4. Geometrical configurations of the lowest energy isomers of FeO_8 and its anion together with the energy shifts with respect to the neutral ground state with $2S + 1 = 1$.

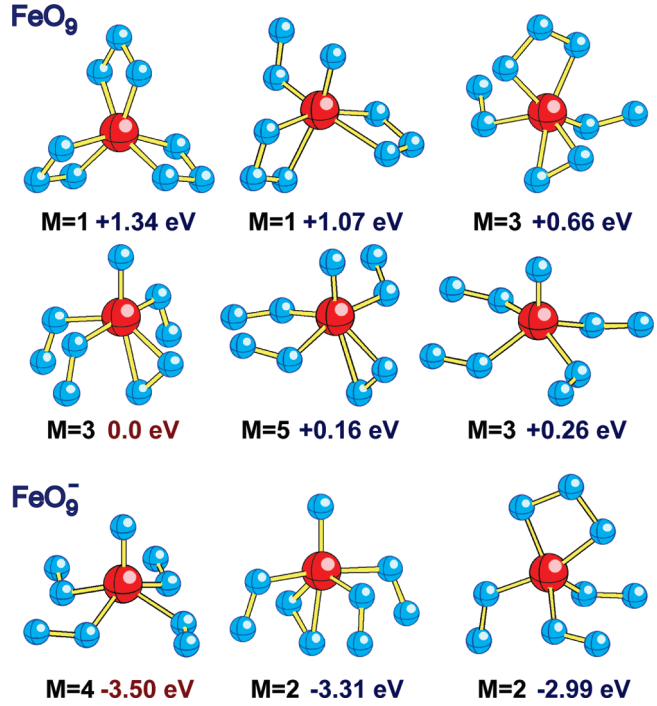

Figure 5. Geometrical configurations of the lowest energy isomers of FeO_9 and its anion together with the energy shifts with respect to the neutral ground state with $2S + 1 = 3$.

by 1.07 and 1.34 eV, respectively. The lowest state of the anion is a quartet, and its nuclear frame contains four superoxo groups.

The most stable states of FeO_{10} contain two peroxo and three superoxo groups, and their total energies are close to each other

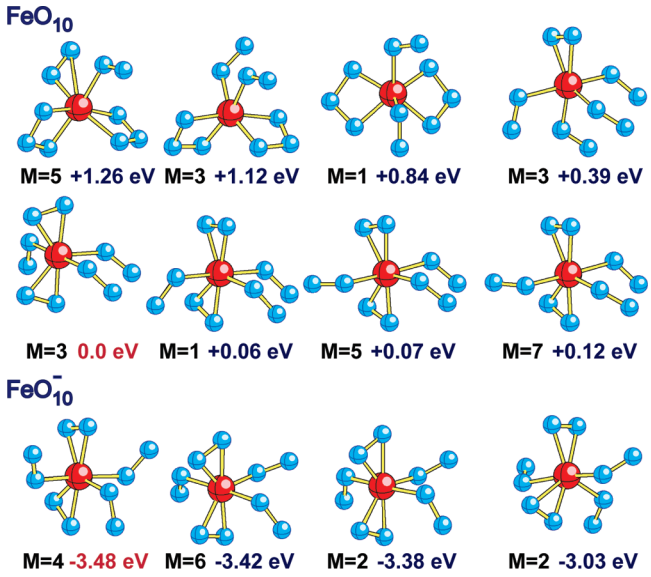

Figure 6. Geometrical configurations of the lowest energy isomers of FeO_{10} and its anion together with the energy shifts with respect to the neutral ground state with $2S + 1 = 3$.

(see Figure 6); namely, the difference in total energy is only 0.12 eV when the spin multiplicity changes from 1 to 7. In the anion series, this difference is larger (0.45 eV). A transformation of one peroxo group into a superoxo group requires ~0.39 eV. The states with the geometrical configurations containing biozonides are higher in total energy with respect to the ground state by ~1 eV. No stable state with an oxo-geometry is found.

Our search for geometrically stable configurations of FeO_{11} and FeO_{11}^- revealed only a few possible geometrical configurations (see Figure 7). They include one with five superoxo groups and another with two peroxo and two ozonide group. Both types of ozone attachment are realized in an anion isomer with $2S + 1 = 6$. Spin excitations of the lowest energy neutral and anion states lead to their decay that releases one (anion) or two (neutral) dioxygens.

We found three types of superoxo isomers for FeO_{12} and FeO_{12}^- shown in Figure 8. They are stable toward spontaneous dissociation in a wide range of spin multiplicities except for the isomers in the third column: the neutral singlet state spontaneously decays to $FeO_{10} + O_2$, whereas the geometry of the corresponding anion isomer with $2S + 1 = 2$ converged during optimizations to the geometry of isomers in the middle column.

Spin Contamination. Often, the quality of computations is evaluated based on the magnitude of spin contamination which is defined by the deviation of the total spin angular momentum expectation value $\langle S^2 \rangle$ from the exact value of $S(S + 1)$. S^2 is a two-particle property and is determined for a N-electron system according to Löwdin[39] as

$$\langle S^2 \rangle = \frac{N(N-4)}{4} + \int \Gamma(\mathbf{r}_1 s_1, \mathbf{r}_2 s_2 | \mathbf{r}_1 s_2, \mathbf{r}_2 s_1) d\mathbf{x}_1 \, d\mathbf{x}_2 \quad (1)$$

where $\mathbf{x}_i = (\mathbf{r}_i, \sigma_i)$ is the combined spatial r_i and spin σ_i coordinate of electron i, and $\Gamma(\mathbf{x}_1', \mathbf{x}_2' | \mathbf{x}_1, \mathbf{x}_2)$ is the two-particle density matrix normalized to $N(N-1)/2$

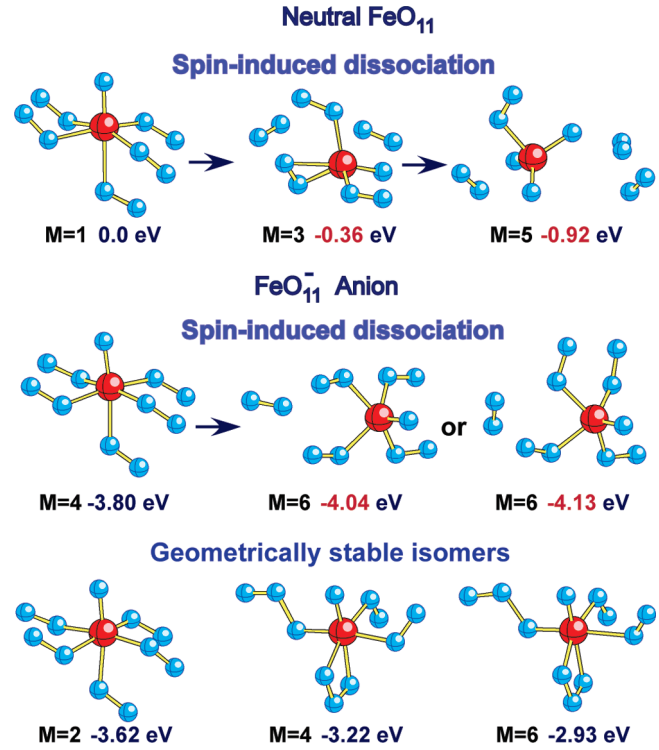

Figure 7. A geometrical configuration of the lowest energy singlet state of FeO_{11} and three configurations of its anion together with the energy shifts with respect to the neutral ground state with $2S + 1 = 1$.

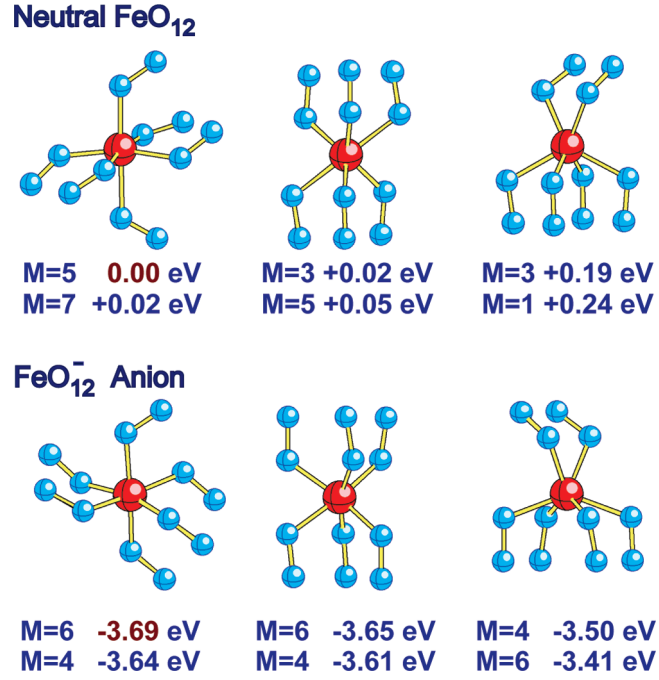

Figure 8. Superoxo configurations of the lowest energy isomers of FeO_{12} and its anion together with the energy shifts with respect to the neutral ground state with $2S + 1 = 5$.

$$\Gamma(\mathbf{x}_1', \mathbf{x}_2' | \mathbf{x}_1, \mathbf{x}_2') = \frac{N(N-1)}{2} \int \Psi(\mathbf{x}_1', ..., \mathbf{x}_N' | \mathbf{x}_1, ..., \mathbf{x}_N) d\mathbf{x}_3 ... d\mathbf{x}_N \quad (2)$$

This two-particle density matrix can be expanded[40] in terms of one-particle density matrices as

$$\Gamma(\mathbf{x}_1',\mathbf{x}_2'|\mathbf{x}_1,\mathbf{x}_2') = \frac{1}{2}[\gamma(\mathbf{x}_1'|\mathbf{x}_1)\gamma(\mathbf{x}_2'|\mathbf{x}_2) - \gamma(\mathbf{x}_1'|\mathbf{x}_2')\gamma(\mathbf{x}_2'|\mathbf{x}_1')] + \Theta(\mathbf{x}_1',\mathbf{x}_2'|\mathbf{x}_1,\mathbf{x}_2) \quad (3)$$

where $\Theta(\mathbf{x}_1',\mathbf{x}_2'|\mathbf{x}_1,\mathbf{x}_2)$ is a unknown modification term.

Density functional theory[41] operates with one-particle electronic densities built from Kohn−Sham (KS) orbitals. These KS orbitals can be used for constructing a unrestricted (UKS) determinantal wave function by analogy with a unrestricted Hartee-Fock determinantal wave function. However, such a UKS wave function corresponds to a fictitious noninteracting system with the same charge density, not a real interacting system. Therefore, the determination of $\langle S^2\rangle$ using UKS determinantal wave functions may not reflect the true spin contamination. Several models[42,43] of estimating the Θ contribution from eq 3 have been discussed and tested for atoms and diatomic molecules. This is found to be a very difficult problem, which is practically equivalent to the unsolved problem of a wave function reconstruction from the known electronic densities.

In most sp-systems, the spin contamination computed from UKS determinants is rather small. This usually is the case when the local excess spin densities are parallel. An antiparralel spin coupling of local excess spin densities is quite common in low-spin states of systems containing transition metal atoms. As an example, we consider FeO_{12} computed in the present work which possesses geometrically stable isomers up to $2S + 1 = 13$.

The state with $2S + 1 = 13$ has $\langle S^2\rangle = 42.027$ and its projection $\langle S^2\rangle A = 42.000$ matches the exact value of $S(S + 1) = 42$. A state with $2S + 1 = 7$ has $\langle S^2\rangle = 13.375$ and $\langle S^2\rangle A = 12.560$, which have to be compared to the exact value of 12. That is, there is a significant difference with respect to the previous high-spin case. The Mulliken population analysis shows that all local spin densities are coupled parallel in the $2S + 1 = 13$ state, whereas the excess spin density at Fe is coupled aniparallel to the excess spin densities at oxygen atoms in the $2S + 1 = 7$ state. The deviation of $\langle S^2\rangle$ from the exact value is the largest in a singlet state where $\langle S^2\rangle = 3.588$ (the exact value is 0) and the projection makes it even worse, $\langle S^2\rangle A = 12.264$, in accordance with Wittbrodt and Schlegel's warning[44] that the spin projection of UKS determinantal wave functions can yield poor results.

The FeO_{12} behavior is rather typical for transition metal compounds. This means that UKS determintal wave functions do present a poor approximation to the wave functions corresponding to interacting system with antiparallel couplings of local excess spin densities.

Vibrational Frequencies. Harmonic vibrational frequencies of the lowest energy states of FeO_n and FeO_n^- are shown in Table 2 for $n = 4$, 5, 6, 8, and 12. These results illustrate the general trend when the number of oxygen atoms is increased. One can see the decrease in the frequency values at the lower energy side and no serious change at the higher energy side. This decrease apparently reflects the increasing floppiness as n grows, whereas the nearly equal frequency values are to be related to small changes in the equilibrium distances of superoxo groups. In order to have a reference frequency, we computed O_2 and its anion in their ground states $^3\Sigma_g^-$ and $^2\Pi_g$ at the same BPW91/6-311+G(3df) level and obtained: O_2: $r_e = 1.218$ Å and $\omega_e = 1557$ cm^{-1} (experimental values[45] are: $r_e = 1.207$ Å and $\omega_e = 1563$ cm^{-1}); O_2^-: $r_e = 1.357$ Å and $\omega_e = 1117$ cm^{-1}. Vibrational frequencies corresponding to superoxo groups in FeO_{12} are 1262, 1282, 1296, 1335, 1343, and 1395 cm^{-1}, and the average O−O bond length is 1.24−1.26 Å, which is closer to the bond length in free O_2 than in the free anion. According to the natural bond orbital (NBO) analysis,[46] which is based on the use of natural atomic orbitals, the effective electronic configuration of Fe in FeO_{12} is $3d^{6.56}4s^{0.29}$, that is, ∼1.15e is transferred to peroxo groups. The NBO data show that this transferred charge is predominantly distributed over oxygen atoms of the first coordination sphere. Thus, this charge transfer appears to lead to the decrease in the superoxo-group frequencies.

Electron Affinity. Adiabatic electron affinities computed using both 6-311+G* and 6-311+G(3df) basis sets are presented in Table 3. As is seen, the EA_{ad} decreases somewhat when the larger basis is used but remains to be larger than the electron affinity of 3.399 ± 0.003 eV[47] of fluorine atom, except for FeO_3 and FeO_8. Therefore, these monoiron oxides are to be considered as weak superhalogens, although only FeO_5 may be considered as satisfying the superhalogen formula[48] for MX_k compounds. This formula requires the sum of normal valencies of X's to be larger than the maximum formal valence of the central atom by one. In the case of FeO_n, Fe has the maximum formal valence of 8, since its valence electronic configuration is $3d^64s^2$, and the normal valence of O is 2. If we accept that the formal valence of superoxo O_2 to be 1, then FeO_5 has to be a superhalogen. Indeed, it has the largest EA_{ad} among all iron oxides presented in Table 3.

The EA_{ad} of O_2 computed at the BPW91/6-311+G(3df) level is 0.415 eV, which is close to the EA_{ad} value of 0.405 eV computed[49] at the CCSD[T] level using a very large aug-pV6Z basis set and to the experimental value[50] of 0.448 ± 0.006 eV. Since the EA_{ad} of dioxygen is rather small, it is quite surprising that the EA_{ad} of iron oxides containing peroxo or superoxo groups is much larger and is nearly independent of the number of oxygen atoms. In order to find an explanation why FeO_n do possess large EA_{ad} values, we analyzed the NBO data for the FeO_{12}^- anion. The effective electronic configuration of Fe in the anion is practically the same as it is in the FeO_{12} neutral, namely, $3d^{6.61}4s^{0.29}$; the excess spin density on each of six oxygen atoms of the first coordination sphere is ∼0.22 e and that of on each outermost oxygen atom is ∼0.11 eV. Thus, the extra electron is distributed over a large number of oxygen atoms in the presence of a positive charge of +1.1e at the central atom. No doubly charged species, which are stable to the second extra electron autodetachment, are found in the series of iron oxides considered.

Thermodynamic Stability. To estimate stability of the iron oxides toward dissociation, we have computed the energies of decay through different channels. These energies were obtained as the difference in total energies of the initial state and the sum of total energies of the decay fragments corrected for the corresponding ZPVEs. The dissociation energies through the channels that yield O, O_2, and O_3 are collected in Tables 4 (neutrals) and 5 (anions). As is seen, both FeO_4 and FeO_4^- are rather stable against dissociation, whereas all other species, except for FeO_9, are unstable toward dissociation of O_2. The largest release of energy is expected to occur during the dissociation of FeO_{12} and FeO_{12}^- to $FeO_4 + 4O_2$ and $FeO_4^- + 4O_2$, respectively. In this case, the released energy is the same in the neutral and the anion because the EA_{ad} values of FeO_4 and FeO_{12} match each other (see Table 3). Since vibrational frequencies for all states, whose dissociation energies are presented in the tables, contain no imaginary frequencies, these states correspond to local minima and there have to be the barriers toward dissociation.

Spontaneous dissociation of superoxo groups observed during our geometry optimizations of FeO_n took place in those cases

TABLE 2: Harmonic Vibrational Frequencies of FeO_n and FeO_n^- in Their Lowest Energy States for $n = 4$, 5, 8, and 12[a]

n	neutral	anion
4	357(2), 408(3), 885, 960(3)	274, 335(2), 339, 394, 833, 867(2), 901
5	68, 155, 197, 230, 234, 275, 359, 460, 822, 886, 994, 1351	118, 155, 244, 264, 311, 328, 339, 508, 841, 892, 906, 1196
6	96, 118, 146, 165, 224, 227, 261, 269, 323, 425, 484, 918, 1013, 1262, 1323	106, 120, 164, 180, 212, 219, 247, 280, 314, 487, 533, 870, 913, 1134, 1191
8	74, 134, 143, 184, 197, 216, 219, 243, 251, 270, 316, 391, 431, 458, 472, 563, 659, 1114, 1120, 1164, 1319	79, 90, 114, 126, 138, 153, 194, 203, 209, 226, 265, 341, 408, 425, 459, 502, 567, 970, 997, 1180, 1233
12	35, 50, 60, 73, 77, 95, 108, 116, 130,148, 159, 173, 185, 197, 198, 229, 244, 249, 282, 319, 349, 369, 375, 388, 404, 435, 524, 1262, 1282, 1296, 1335, 1343, 1396	48, 58, 77, 97,111, 119, 130, 145, 162,171, 187, 193, 212, 218, 225, 234, 262, 266, 271, 288, 318, 379, 389, 410, 432, 442, 459, 1168, 1197, 1214, 1230, 1259, 1307

[a] All values are in cm^{-1}; numbers in the parentheses for $n = 4$ stand for the degeneracy of the corresponding mode; O_2 ($^3\Sigma_g$) $\omega_e = 1557$ cm^{-1}; O_2^- ($^2\Pi_g$) $\omega_e = 1117$ cm^{-1} at the same BPW91/6-311+G(3df) level.

TABLE 3: Adiabatic Electron Affinities of FeO_n Computed at the BPW91 Level of Theory Using two Basis Sets[a]

	6-311+G*	6-311+G(3df)
FeO_3	3.33	3.25[b]
FeO_4	3.79	3.69[c]
FeO_5	4.15	3.95
FeO_6	3.78	3.56
FeO_7	3.59	3.57
FeO_8	3.54	3.24
FeO_9	3.85	3.50
FeO_{10}	3.52	3.48
FeO_{11}	3.84	3.80
FeO_{12}	3.76	3.69

[a] All values are in eV. [b] Experimental value is 3.31 ± 0.06 eV, see ref 6h. [c] Experimental value is 3.84 ± 0.04 eV (the vertical detachment energy), see ref 6h.

TABLE 4: Dissociation Energies of FeO_n Through Different Decay Channels[a]

channel	D_0	channel	D_0
$FeO_4 \rightarrow FeO_2 + O_2$	1.88	$FeO_9 \rightarrow FeO_7 + O_2$	0.15
$\rightarrow FeO_3 + O$	3.21	$\rightarrow FeO_6 + O_3$	1.17
$FeO_5 \rightarrow FeO_3 + O_2$	0.03	$\rightarrow FeO_8 + O$	3.14
$\rightarrow FeO_4 + O$	2.72	$FeO_{10} \rightarrow FeO_8 + O_2$	**−0.01**
$\rightarrow FeO_2 + O_3$	3.11	$\rightarrow FeO_4 + 3O_2$	**−0.93**
$FeO_6 \rightarrow FeO_4 + O_2$	**−0.50**	$\rightarrow FeO_9 + O$	2.76
$\rightarrow FeO_5 + O$	2.68	$FeO_{11} \rightarrow FeO_9 + O_2$	**−0.69**
$FeO_7 \rightarrow FeO_5 + O_2$	**−0.65**	$\rightarrow FeO_4 + 2O_2 + O_3$	0.04
$\rightarrow FeO_4 + O_3$	0.58	$\rightarrow FeO_8 + O_3$	0.96
$\rightarrow FeO_6 + O$	2.57	$\rightarrow FeO_{10} + O$	2.46
$FeO_8 \rightarrow FeO_6 + O_2$	**−0.42**	$FeO_{12} \rightarrow FeO_{10} + O_2$	**−0.56**
$\rightarrow FeO_4 + 2O_2$	**−0. 92**	$\rightarrow FeO_4 + 4O_2$	**−1.48**
$\rightarrow FeO_7 + O$	2. 91	$\rightarrow FeO_{11} + O$	2.89

[a] All values are in eV.

TABLE 5: Dissociation Energies of FeO_n^- Through Different Decay Channels[a]

channel	D_0	channel	D_0
$FeO_4^- \rightarrow FeO_2^- + O_2$	3.35	$FeO_9^- \rightarrow FeO_7^- + O_2$	0.09
$\rightarrow FeO_3^- + O$	3.65	$\rightarrow FeO_6^- + O_3$	1.06
$FeO_5^- \rightarrow FeO_3^- + O_2$	0.77	$\rightarrow FeO_8^- + O$	3.34
$\rightarrow FeO_4^- + O$	3.02	$FeO_{10}^- \rightarrow FeO_4^- + 3O_2$	**−1.13**
$\rightarrow FeO_2^- + O_3$	4.88	$\rightarrow FeO_8^- + O_2$	0.17
$FeO_6^- \rightarrow FeO_4^- + O_2$	**−0.52**	$\rightarrow FeO_9^- + O$	2.73
$\rightarrow FeO_5^- + O$	2.40	$FeO_{11}^- \rightarrow FeO_9^- + O_2$	**−0.40**
$FeO_7^- \rightarrow FeO_5^- + O_2$	**−1.08**	$\rightarrow FeO_4^- + 2O_2 + O_3$	0.14
$\rightarrow FeO_4^- + O_3$	0.45	$\rightarrow FeO_8^- + O_3$	1.45
$\rightarrow FeO_6^- + O$	2.47	$\rightarrow FeO_{10}^- + O$	2.77
$FeO_8^- \rightarrow FeO_6^- + O_2$	**−0.78**	$FeO_{12}^- \rightarrow FeO_{10}^- + O_2$	**−0.34**
$\rightarrow FeO_4^- + 2O_2$	**−1.30**	$\rightarrow FeO_4^- + 4O_2$	**−1.48**
$\rightarrow FeO_7^- + O$	2.65	$\rightarrow FeO_{11}^- + O$	2.79

[a] All values are in eV.

when a trial geometrical configuration included as a fragment the lowest energy state of FeO_{n-2}, and the decay is not spin-forbidden (see Figure 1, the FeO_5^- series and Figure 7, the FeO_{11}^- series). As shown in the top panel of Figure 7, the spin excitations can initiate the cascade release of dioxygen.

Summary

The results of our computations performed using density functional theory with generalized gradient approximation (DFT-GGA) for the neutral and negatively charged FeO_n species show that there are geometrically stable isomers for each n in the range from $n = 5$ to 12. The isomer states do correspond to local minima and are unstable toward release of dioxygen for $n > 5$. All the neutral species do possess rather large electron affinities ranging from 3.24 to 3.95 eV, and the anions can potentially serve as counterions in salts if a proper cation is found. Such salts would possess a high oxidative power.

Acknowledgment. This research was supported by a grant from the Defense Threat Reduction Agency (Grant No. HDTRA1-09-1-0025). C. A. W. was partly supported by the NSF CREST Cooperative Agreement HRD-0630370. The research was also supported in part by the National Science Foundation through TeraGrid resources provided by NCSA. Portions of this research were conducted with high performance computational resources provided by the Louisiana Optical Network Initiative (http://www.loni.org).

Supporting Information Available: Tables containing vibrational frequencies and the corresponding intensities for all lowest energy states in the neutral and anionic series of FeO_n ($n = 4-12$) together with the corresponding $\langle S^2 \rangle$ and $\langle S^2 \rangle A$ values are provided. This material is available free of charge via the Internet at http://pubs.acs.org.

References and Notes

(1) (a) Gong, Y.; Zhou, M.; Andrews, L. *Chem. Rev.* **2009**, *109*, 6765. (b) Jena, P.; Castleman, A. W., Jr. *Proc. Natl. Acad. Sci. U.S.A* **2006**, *103*, 10560.

(2) (a) Xue, W.; Wang, Z.-C.; He, S.-G.; Xie, Y.; Bernstein, E. R. *J. Am. Chem. Soc.* **2008**, *30*, 15879. (b) Reilly, N. M.; Reveles, J. U.; Johnson, G. E.; del Campo, J. M.; Khanna, S. N.; Kolster, A. M.; Castleman, A. W., Jr. *J. Phys. Chem. C* **2007**, *111*, 19086. (c) Šmit, G.; Zrnčeviæ, S.; Lázárc., K. *Mol. Cat. A* **2006**, *252*, 103. (d) Reddy, B. V.; Khanna, S. N. *Phys. Rev. Lett.* **2004**, *93*, 068301. (e) Gutsev, G. L.; Bauschlicher, C. W., Jr. *Chem. Phys. Lett.* **2003**, *380*, 435. (f) Li, P.; Miser, D. E.; Rabiei, S.; Yadav, R. T. *Appl. Catal., B* **2003**, *43*, 151.

(3) Steinfeld, A.; Sanders, S.; Palumbo, R. *Solar Energy* **1999**, *65*, 43.

(4) (a) Weiller, B. H.; Bechthold, P. S.; Parks, E. K.; Pobo, L. G.; Riley, S. J. *J. Chem. Phys.* **1989**, *91*, 4714. (b) Gutsev, G. L.; Mochena, M. D.; Bauschlicher, C. W., Jr. *Chem. Phys.* **2005**, *314*, 291.

(5) Mebel, A. M.; Hwang, D. Y. *J. Phys. Chem. A* **2001**, *105*, 7460.
(6) (a) Chestakov, D. A.; Parker, D. H.; Baklanov, A. V. *J. Chem. Phys.* **2005**, *122*, 084302. (b) Metz, R. B.; Nicolas, C.; Ahmed, M.; Leone, S. R. *J. Chem. Phys.* **2005**, *123*, 114313. (c) Son, H. S.; Lee, K.; Shin, S. K.; Ku, J. K. *Chem. Phys. Lett.* **2000**, *320*, 658. (d) Drechsler, G.; Boesl, U.; Bässmann, C.; Schlag, E. W. *J. Chem. Phys.* **1997**, *107*, 2284. (e) Allen, M. D.; Ziurys, L. M.; Brown, J. M. *Chem. Phys. Lett.* **1996**, *257*, 130. (f) Chertihin, G. V.; Saffel, W.; Yustein, J. T.; Andrews, L.; Neurock, M.; Ricca, A.; Bauschlicher, C. W., Jr. *J. Phys. Chem.* **1996**, *100*, 5261. (g) Wu, H. B.; Desai, S. R.; Wang, L. S. *J. Am. Chem. Soc.* **1996**, *118*, 5296. (h) Wu, H. B.; Desai, S. R.; Wang, L. S. *J. Am. Chem. Soc.* **1996**, *118*, 7434. (i) Fan, J.; Wang, L. S. *J. Chem. Phys.* **1995**, *102*, 8714. (j) Steimle, T. C.; Nachman, D. F.; Shirley, J. E.; Merer, A. J. *J. Chem. Phys.* **1989**, *90*, 5360. (k) Andersen, T.; Lykke, K. R.; Neumark, D. M.; Lineberger, W. C. *J. Chem. Phys.* **1987**, *86*, 1858. (l) Kröckertskothen, T.; Knöckel, H.; Tiemann, E. *Mol. Phys.* **1987**, *62*, 1031. (m) Taylor, A. W.; Cheung, A. S.-C.; Merer, A. J. *J. Mol. Spectrosc.* **1985**, *113*, 487. (n) Cheung, A. S.-C.; Lee, N.; Lyyra, A. M.; Merer, A. J.; Taylor, A. W. *J. Mol. Spectrosc.* **1982**, *95*, 213. (o) Cheung, A. S. C.; Gordon, R. M.; Merer, A. J. *J. Mol. Spectrosc.* **1981**, *87*, 289. (p) Harris, S. M.; Barrow, R. F. *J. Mol. Spectrosc.* **1980**, *84*, 334. (q) Green, D. W.; Reedy, G. T.; Kay, J. G. *J. Mol. Spectrosc.* **1979**, *78*, 257. (r) Engelking, P. C.; Lineberger, W. C. *J. Chem. Phys.* **1977**, *66*, 5054. (s) West, J. B.; Broida, H. P. *J. Chem. Phys.* **1975**, *62*, 2566.
(7) (a) Baranowska, A.; Siedlecka, M.; Sadlej, A. J. *Theor. Chem. Acc.* **2007**, *118*, 959. (b) Jensen, K. P.; Roos, B. O.; Ryde, U. *J. Chem. Phys.* **2007**, *126*, 14103. (c) Uzunova, E. L.; Nikolov, G. St.; Mikosch, H. *ChemPhysChem* **2004**, *5*, 192. (d) Shiroishi, H.; Oda, T.; Hamada, I.; Fujima, N. *Eur. Phys. J., D* **2003**, *24*, 85. (e) Dai, B.; Deng, K. M.; Yang, J. L.; Zhu, Q. S. *J. Chem. Phys.* **2003**, *118*, 9608. (f) Gutsev, G. L.; Andrews, L.; Bauschlicher, C. W., Jr. *Theor. Chem. Acc.* **2003**, *109*, 298. (g) Bridgeman, A. J.; Rothery, J. *J. Chem. Soc., Dalton Trans.* **2000**, 211. (h) Gutsev, G. L.; Rao, B. K.; Jena, P. *J. Phys. Chem. A* **2000**, *104*, 5374. (i) Gutsev, G. L.; Khanna, S. N.; Rao, B. K.; Jena, P. *J. Phys. Chem. A* **1999**, *103*, 5812. (j) Glukhovtsev, M. N.; Bach, R. D.; Nagel, C. J. *J. Phys. Chem. A* **1997**, *101*, 316. (k) Bakalbassis, E. G.; Stiakaki, M. A. D.; Tsipis, A. C.; Tsipis, C. A. *Chem. Phys.* **1996**, *205*, 389. (l) Bauschlicher, C. W., Jr.; Maitre, P. *Theor.Chim. Acta* **1995**, *90*, 189. (m) Bauschlicher, C. W., Jr.; Langhoff, S. R.; Komornicki, A. *Theor. Chim. Acta* **1990**, *77*, 263. (n) Anderson, A. B.; Hong, S. Y.; Smialek, J. L. *J. Phys. Chem.* **1987**, *91*, 4250. (o) Anderson, A. B.; Grimes, R. W.; Hong, S. Y. *J. Phys. Chem.* **1987**, *91*, 4245. (p) Dolg, M.; Wedig, U.; Stoll, H.; Preuss, H. *J. Chem. Phys.* **1987**, *86*, 2123. (q) Krauss, M.; Stevens, W. J. *J. Chem. Phys.* **1985**, *82*, 5584. (r) Blyholder, G.; Head, J.; Ruette, F. *Inorg. Chem.* **1982**, *21*, 1539. (s) Bagus, P. S.; Preston, H. J. T. *J. Chem. Phys.* **1973**, *59*, 2986.
(8) Hendrickx, M. F. A.; Anam, K. R. *J. Phys. Chem. A* **2009**, *113*, 8746.
(9) Neumark, D. M.; Lineberger, W. C. *J. Phys. Chem. A* **2009**, *113*, 10588.
(10) (a) Gong, Y.; Zhou, M. F.; Andrews, L. *J. Phys. Chem. A* **2007**, *111*, 12001. (b) Chertihin, G. V.; Saffel, W.; Yustein, J. T.; Andrews, L.; Neurock, M.; Ricca, A.; Bauschlicher, C. W., Jr. *J. Phys. Chem.* **1996**, *100*, 5261. (c) Andrews, L.; Chertihin, f. V.; Ricca, A.; Bauschlicher, C. W., Jr. *J. Am. Chem. Soc.* **1996**, *118*, 467. (d) Fanfarillo, M.; Downs, A. J.; Green, T. M.; Almond, M. J. *Inorg. Chem.* **1992**, *31*, 2973. (e) Chang, S.; Blyholder, G.; Fernandez, J. *Inorg. Chem.* **1981**, *20*, 2813. (f) Abramowitz, S.; Acquista, N.; Levin, I. W. *Chem. Phys. Lett.* **1977**, *50*, 423.
(11) Yamada, Y.; Sumino, H.; Okamura, Y.; Shimasaki, H.; Tominaga, T. *Appl. Radiat. Isot.* **2000**, *52*, 157.
(12) (a) Grein, F. *Int. J. Quantum Chem.* **2009**, *109*, 549. (b) Uzunova, E. L.; Mikosch, H.; Nikolov, G. *J. Chem. Phys.* **2008**, *128*, 094307. (c) Gutsev, G. L.; Rao, B. K.; Jena, P. *J. Phys. Chem. A* **2000**, *104*, 11961. (d) García-Sosa, A. T.; Castro, M. *Int. J. Quantum Chem.* **2000**, *80*, 307. (e) Kellogg, C. B.; Irikura, K. K. *J. Phys. Chem. A* **1999**, *103*, 1150. (g) Cao, Z.; Duran, M.; Solà, M. *Chem. Phys. Lett.* **1997**, *274*, 411. (f) Lyne, P. D.; Mingos, D. M. P.; Ziegler, T.; Downs, A. J. *Inorg. Chem.* **1993**, *32*, 4785.
(13) Gong, Y.; Zhou, M. F. *J. Phys. Chem. A* **2008**, *112*, 10838.
(14) (a) Gong, Y.; Zhou, M. F. *J. Phys. Chem. A* **2008**, *112*, 10838. (b) Rollason, R. J.; Plane, J. M. C. *Phys. Chem. Chem. Phys.* **2000**, *2*, 2335.
(15) (a) Gutsev, G. L.; Khanna, S. N.; Rao, B. K.; Jena, P. *Phys. Rev. A* **1999**, *59*, 3681. (b) Atanasov, M. *Inorg. Chem.* **1999**, *38*, 4942.
(16) Cao, Z.; Wu, W.; Zhang, Q. *THEOCHEM* **1999**, *489*, 165.
(17) Riedela, S.; Kaupp, M. *Coord. Chem. Rev.* **2009**, *253*, 606.
(18) Wu, H.; Desai, R.; Wang, L. S. *J. Phys. Chem.A* **1997**, *101*, 2103.
(19) (a) Pouillon, Y.; Massobrio, C. *Chem. Phys. Lett.* **2002**, *356*, 469. (b) Massobrio, C.; Pouillon, Y. *J. Chem. Phys.* **2003**, *119*, 8305. (c) Baruah, T.; Zope, R. R.; Pederson, M. R. *Phys. ReV. A* **2004**, *69*, 023201.
(20) Gong, Y.; Zhou, M. *Phys. Chem. Chem. Phys.* **2009**, *11*, 8714.
(21) Gong, Y.; Ding, C.; Zhou, M. *J. Phys. Chem. A* **2007**, *111*, 11572.
(22) Shiroishi, H.; Oda, T.; Hamada, I.; Fujima, N. *Eur. Phys. J., D* **2003**, *24*, 85.
(23) Frisch, M. J.; Trucks, G. W.; Schlegel, H. B.; Scuseria, G. E.; Robb, M. A.; Cheeseman, J. R.; Montgomery, J. A., Jr.; Vreven, T.; Kudin, K. N.; Burant, J. C.; Millam, J. M.; Iyengar, S. S.; Tomasi, J.; Barone, V.; Mennucci, B.; Cossi, M.; Scalmani, G.; Rega, N.; Petersson, G. A.; Nakatsuji, H.; Hada, M.; Ehara, M.; Toyota, K.; Fukuda, R.; Hasegawa, J.; Ishida, M.; Nakajima, T.; Honda, Y.; Kitao, O.; Nakai, H.; Klene, M.; Li, X.; Knox, J. E.; Hratchian, H. P.; Cross, J. B.; Bakken, V.; Adamo, C.; Jaramillo, J.; Gomperts, R.; Stratmann, R. E.; Yazyev, O.; Austin, A. J.; Cammi, R.; Pomelli, C.; Ochterski, J. W.; Ayala, P. Y.; Morokuma, K.; Voth, G. A.; Salvador, P.; Dannenberg, J. J.; Zakrzewski, V. G.; Dapprich, S.; Daniels, A. D.; Strain, M. C.; Farkas, O.; Malick, D. K.; Rabuck, A. D.; Raghavachari, K.; Foresman, J. B.; Ortiz, J. V.; Cui, Q.; Baboul, A. G.; Clifford, S.; Cioslowski, J.; Stefanov, B. B.; Liu, G.; Liashenko, A.; Piskorz, P.; Komaromi, I.; Martin, R. L.; Fox, D. J.; Keith, T.; Al-Laham, M. A.; Peng, C. Y.; Nanayakkara, A.; Challacombe, M.; Gill, P. M. W.; Johnson, B.; Chen, W.; Wong, M. W.; Gonzalez, C.; Pople, J. A. *Gaussian 03, Revision D.01*; Gaussian, Inc.: Pittsburgh PA, 2003.
(24) Curtiss, L. A.; McGrath, M. P.; Blaudeau, J.-P.; Davis, N. E.; Binning, R. C., Jr.; Radom, L. *J. Chem. Phys.* **1995**, *103*, 6104.
(25) Becke, A. D. *Phys. Rev. A* **1988**, *38*, 3098.
(26) Perdew, J. P.; Wang, Y. *Phys. Rev. B* **1992**, *45*, 13244.
(27) Perdew, J. P.; Burke, K.; Ernzerhof, M. *Phys. Rev. Lett.* **1996**, *77*, 3865.
(28) Becke, A. D. *J. Chem. Phys.* **1993**, *98*, 5648.
(29) Lee, C.; Yang, W.; Parr, R. G. *Phys. Rev. B* **1988**, *37*, 785.
(30) Stephens, P. J.; Devlin, F. J.; Chabalowski, C. F.; Frisch, M. J. *J. Phys. Chem.* **1994**, *98*, 11623.
(31) Tao, J. M.; Perdew, J. P.; Staroverov, V. N.; Scuseria, G. E. *Phys. Rev. Lett.* **2003**, *91*, 146401.
(32) (a) Dunning, T. H., Jr. *J. Chem. Phys.* **1989**, *90*, 1007, for O. (b) Balabanov, N. B.; Peterson, K. A. *J. Chem. Phys.* **2005**, *123*, 064107, for Fe.
(33) (a) Casida, M. E.; Jamorski, C.; Casida, K. C.; Salahub, D. R. *J. Chem. Phys.* **1998**, *108*, 4439. (b) Burke, K.; Werschnik, J.; Gross, E. K. U. *J. Chem. Phys.* **2005**, *123*, 062206. (c) Wang, F.; Ziegler, T.; van Lenthe, E.; van Gisbergen, S.; Baerends, E. J. *J. Chem. Phys.* **2005**, *123*, 204103.
(34) Gutsev, G. L.; Mochena, M. D.; Bauschlicher, C. W., Jr. *J. Phys. Chem. A* **2003**, *107*, 7013.
(35) Gutsev, G. L.; O'Neal, R. H., Jr.; Saha, B. C.; Mochena, M. D.; Johnson, E.; Bauschlicher, C. W., Jr. *J. Phys. Chem. A* **2008**, *112*, 10728.
(36) Li, S.; Dixon, D. A. *J. Phys. Chem. A* **2007**, *111*, 11908.
(37) Kaiser, R. I.; Mebel, A. M. *Chem. Phys. Lett.* **2008**, *465*, 1.
(38) (a) Zùchowski, P. S. *Chem. Phys. Lett.* **2008**, *450*, 203. (c) Brown, L.; Vaida, V. *J. Phys. Chem.* **1996**, *100*, 7849.
(39) Löwdin, P.-O. *Phys. Rev.* **1955**, *97*, 1474.
(40) Wang, J.; Becke, A. D.; Smith, V. H., Jr. *J. Chem. Phys.* **1995**, *102*, 3477.
(41) Kohn, W.; Sham, L. J. *Phys. Rev.* **1965**, *140* (4A), A1133.
(42) Gräfenstein, J.; Cremer, D. *Mol. Phys.* **2001**, *99*, 981.
(43) Cohen, A. J.; Tozer, D. J.; Handy, N. C. *J. Chem. Phys.* **2007**, *126*, 214104.
(44) Wittbrodt, J. M.; Schlegel, H. B. *J. Chem. Phys.* **1996**, *105*, 6574.
(45) Huber, K. P.; Herzberg, G. *Constants of Diatomic Molecules*; Van Nostrand-Reinhold: NewYork, 1979.
(46) Reed, A. E.; Curtiss, L. A.; Weinhold, F. *Chem. Rev.* **1988**, *88*, 899.
(47) Hotop, H.; Lineberger, W. C. *J. Phys. Chem. Ref. Data* **1985**, *14*, 731.
(48) (a) Gutsev, G. L.; Boldyrev, A. I. *Chem. Phys. Lett.* **1981**, *84*, 352. (b) Gutsev, G. L.; Boldyrev, A. I. *Chem. Phys.* **1981**, *56*, 277. (c) Gutsev, G. L.; Boldyrev, A. I. *Chem. Phys.* **1983**, *75*, 243. (d) Gutsev, G. L.; Boldyrev, A. I. *Mol. Phys.* **1984**, *11*, 1. (e) Gutsev, G. L.; Boldyrev, A. I. *Adv. Chem. Phys.* **1985**, *61*, 169.
(49) Sulka, M.; Pitonak, P.; Neogrady, P.; Urban, M. *Int. J. Quantum Chem.* **2008**, *108*, 2159.
(50) Ervin, K. M.; Anusiewicz, I.; Skurski, P.; Simons, J.; Lineberger, W. C. *J. Phys. Chem. A* **2003**, *107*, 8521.

JP1050645